Ab initio calculations of arsenic in silicon: Diffusion mechanism and strain dependence

Kilian Vollenweider, Beat Sahli, and Wolfgang Fichtner
Integrated Systems Laboratory, ETH Zurich, Gloriastrasse 35, 8092 Zurich, Switzerland
(Received 27 April 2010; published 26 May 2010)

We investigated the diffusion of arsenic (As) in [100]-uniaxially compressive and tensile stressed silicon with density functional simulations, for stress values up to 1.8 GPa. At a temperature of 1000 °C, the diffusion coefficient of the most prevalent As vacancy pair (As-*V*) was found to be up to eight times higher in compressively strained silicon than in the unstrained case. Under tensile strain, the diffusion coefficient was found to be changed by a factor of maximally 0.8. In molecular dynamics simulations, we observed As-*V* to diffuse via a ring mechanism in relaxed silicon, with a calculated overall energy barrier of 1.29 eV. Poisson's ratio of uniaxially strained silicon in the [100] direction was calculated to be 0.26.

DOI: 10.1103/PhysRevB.81.174119 PACS number(s): 61.72.J−, 62.20.dj, 66.30.J−, 68.55.Ln

I. INTRODUCTION

The ongoing aggressive scaling of semiconductor devices requires ultrashallow junctions. Arsenic, with its high solubility and rather low diffusivity, is the preferred *n*-type dopant for silicon.[1] However, during postimplantation annealing at high concentrations, As exhibits the phenomenon of transient enhanced diffusion, explained by *V*-mediated diffusion.[2,3] A solid understanding of arsenic vacancy pair (As-*V*) diffusion is therefore very important to control the resulting dopant profile spreading. Another challenging task in the fabrication of scaled devices is the improvement of the electrical performance through mobility enhancement. In recent years, strain engineering has established itself as a very successful technique in this regard. Uniaxial strain is preferred in most complementary metal-oxide semiconductor transistor technologies.[4]

In this paper, we present an *ab initio* study of As diffusion in uniaxially strained silicon. First, the elastic behavior of crystalline silicon under compressive and tensile stress was investigated by calculating Poisson's ratio. The obtained result was used for all simulations with strained structures. In a second step, we determined the strain dependence of the relative diffusion coefficient for the most prevalent mobile As defect. From the strain-dependent minimum energy configurations of the four mobile defects *I* (self-interstitial), *V* (vacancy), As-*I* (arsenic interstitial), and As-*V*, the last one was determined as the most numerous defect due to its significantly smaller formation energy. In contrast to previous *ab initio* work on As-*V* diffusion in strained silicon,[5] we examined its diffusion mechanism with molecular dynamics (MD) simulations. Furthermore, all migration steps of the observed ring mechanism were considered. The calculated migration barriers were combined with the formation energies to finally estimate the As-*V* diffusion coefficient.

The density functional simulations were performed with the Vienna ab initio simulation package (VASP).[6,7] The projector augmented wave (PAW) method[8] was used. The cutoff for the plane-wave expansion was set to 300 eV, and the condition for electronic selfconsistency was 10^{-4} eV. Exchange and correlation effects were calculated with the generalized gradient approximation (GGA) (Perdew-Wang 91). The Brillouin zone was sampled only at the Γ point. The atomic structure minimization was performed by the conjugate gradient algorithm. The MD simulations were performed with a time step of 1 fs and in a simulation cell with with 64 ∓ 1 atoms. For nudged elastic band (NEB) simulations, the same supercell was used. The relaxations to determine minimum energy configurations were performed in 216 ∓ 1 atom supercells. In all simulations with unstrained silicon the calculated lattice constant was set to 5.47 Å.

II. RESULTS AND DISCUSSION

A. Poisson ratio of silicon

As preliminary investigation into defect structures of strained silicon, we studied perfect silicon under uniaxial stress. If compressive stress is applied in the [100] direction, the structure is relaxed equally in the two other perpendicular directions. For tensile stress, the crystal contracts equally in those directions. The relation between uniaxial stress (σ_{xx}) and strain (ε_{xx}) in the [100] direction is given by Young's modulus Y_{100}: $\varepsilon_{xx}=\frac{\sigma_{xx}}{Y_{100}}$. The strain resulting in the two symmetrically equivalent perpendicular directions [010] and [001] is given by Poisson's ratio

$$\nu = -\frac{\varepsilon_{\perp}}{\varepsilon_{\parallel}} = -\frac{\varepsilon_{yy}}{\varepsilon_{xx}} = -\frac{\varepsilon_{zz}}{\varepsilon_{xx}}. \quad (1)$$

$Y_{100}=1.3\times10^{12}$ dyn/cm^2 leads to a compressive and tensile strain value of 0.014 for the stress maximum of 1.8 GPa.[9]

The perpendicular strains (ε_{yy} and ε_{zz}) were derived with *ab initio* simulations. We calculated the total energy of perfect silicon for a combination of uniformly distributed strain values (Fig. 1). As theory[10] postulates a quadratic relation between the energy of a linear elastic solid and the applied strain, we fitted the calculated energies to obtain the equation

$$E_{\mathrm{tot}}^{\mathrm{Si}} - E_{\mathrm{ref}}^{\mathrm{Si}}(\mathrm{eV}) = 2157\varepsilon_{xx}^2 + 6077\varepsilon_{yy}^2 + 3214\varepsilon_{xx}\varepsilon_{yy}, \quad (2)$$

and minimized the fit function to ε_{yy} for constant ε_{xx}. In agreement with Eq. (1), this leads to a linear relation of parallel and perpendicular strain. From our calculations, we found Poisson ratio $\nu=0.26$, which agrees very well with other experimental[11] ($\nu=0.27$) and theoretical[9] ($\nu=0.28$) studies.

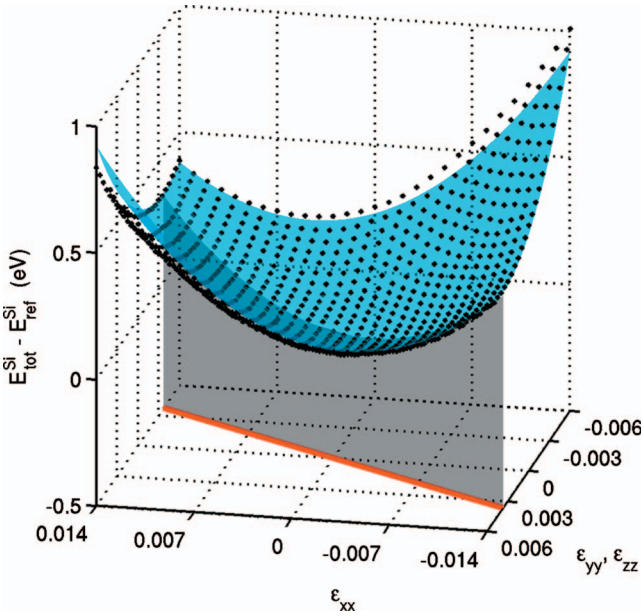

FIG. 1. (Color) The calculated total energies of silicon (black dots) for different combinations of perpendicular and parallel strain and quadratic fit (blue surface). The strain values for which the energies are minimal are represented by the red line.

B. Mobile defects

The minimum energy configurations of the four mobile defects *V*, *I*, As-*I*, and As-*V* were determined with relaxations for each applied strain value. For the interstitial defects, we investigated the two split orientations ⟨110⟩ and ⟨011⟩ because they are not equivalent in uniaxially strained silicon. Each of the four remaining split orientations is symmetrically equivalent to one of them. The coordinate systems of strained structures differ from each other. In order to compare the strain minimum configurations in the same coordinate system, we transformed them into the coordinate system of unstrained silicon. To visualize the 3*N*-dimensional ($N=216\mp1$) configuration space, it was reduced to two dimensions by a classical multidimensional scaling technique.[12] Figure 2 shows the minimum energy configurations in the lattice of perfect unstrained silicon and in the reduced configuration space. Points in the configuration space that are grouped together were regarded as having the same configuration. With this definition, we identified the following three configuration classes:

(1) *Separated,* The configurations of *V* are separated into two groups [Fig. 2(a)], corresponding to different Jahn-Teller distortions for tensile (blue) and compressive (red) strain. The four silicon neighbors of *V* form pairs, which are characterized by atom distances. The two atoms of the same pair are closer to each other than to an atom of the other pair. In compressive silicon the pairs have ⟨110⟩- and $\langle\bar{1}10\rangle$-orientation and in the tensile case they are ⟨011⟩ and $\langle 01\bar{1}\rangle$ oriented.

(2) *Strain independent,* The minimum energy configurations of the interstitial defects are all split configurations that are identical for differently strained silicon [Figs. 2(b)–2(e)].

(3) *Continuously changing,* Although *V* and As atom are direct neighbors in all As-*V* configurations, there are small but continuous changes in configurations for the different strains [Fig. 2(f)].

From these results, we conclude that the minimum energy configurations of defects can change in silicon with different strains. The formation energy calculation of defects in strained silicon is a generalization of the unstrained case.[13,14] The formation energy of a defect *X* in silicon with strain ε is calculated according to

$$E_f^X(\varepsilon) = E_{\text{tot}}^X(\varepsilon) - \sum_i n_i \mu_i(\varepsilon), \tag{3}$$

where $E_{\text{tot}}^X(\varepsilon)$ is the total energy of the strained supercell containing the defect *X* and n_i is the number of atoms of type *i* in the supercell. The corresponding reference energy $\mu_i(\varepsilon)$ is the strained equivalent to $\mu_i(\varepsilon=0)$, defined in Refs. 13 and 14.

For the cases of perfect silicon and silicon with a defect, we assumed that the total energy exhibits a quadratic strain dependence. In combination with Eqs. (1) and (3), similar to earlier work,[15] this assumption permits to express the formation energy of a defect as a quadratic function of the applied uniaxial strain ε_{xx}. The results are presented in Fig. 3.

The formation energies of the two discovered *V* configurations for tensile and compressive strain were reproduced with two fits that coincide for the unstrained case. Compared to the unstrained case, the formation of *V* is increasingly favored for both tensile and compressive strains. The self-interstitial is an additional atom in the bulk and a volume increase supports its formation. An extension of the lattice decreases the formation energy. For tensile strains, the formation of the ⟨110⟩ orientation is favored. For compressive strains, the self-interstitial has ⟨011⟩ orientation. Similarly, the formation energies of both As-*I* orientations decrease when the structure is extended. While the As-*I*⟨110⟩ is favored for compressive strains, none of the orientations is preferred for the tensile case. The formation energies of the different minimum energy configurations of As-*V* were approximated with two fits. Compared to the other mobile defects, the formation energies of As-*V* are significantly smaller (at least 0.5 eV). This agrees with the prevailing opinion in literature[16–18] that As-*V* makes a dominant contribution to As diffusion in silicon.

C. Diffusion mechanism of As-*V*

We analyzed the diffusion mechanism of the As-*V* pair by a systematic combination of MD, relaxations and NEB simu-

TABLE I. Statistics of the MD simulation. Left part: Migration mechanisms and number of visits in a configuration. Right part: Total time spent in a configuration by the vacancy.

Mechanism	Number of events	Configuration	Time (ps)
Exchange	8	NN1	164.0
NN1 ↔ NN2	6	NN2	4.6
NN2 ↔ NN3	1	NN3	1.4

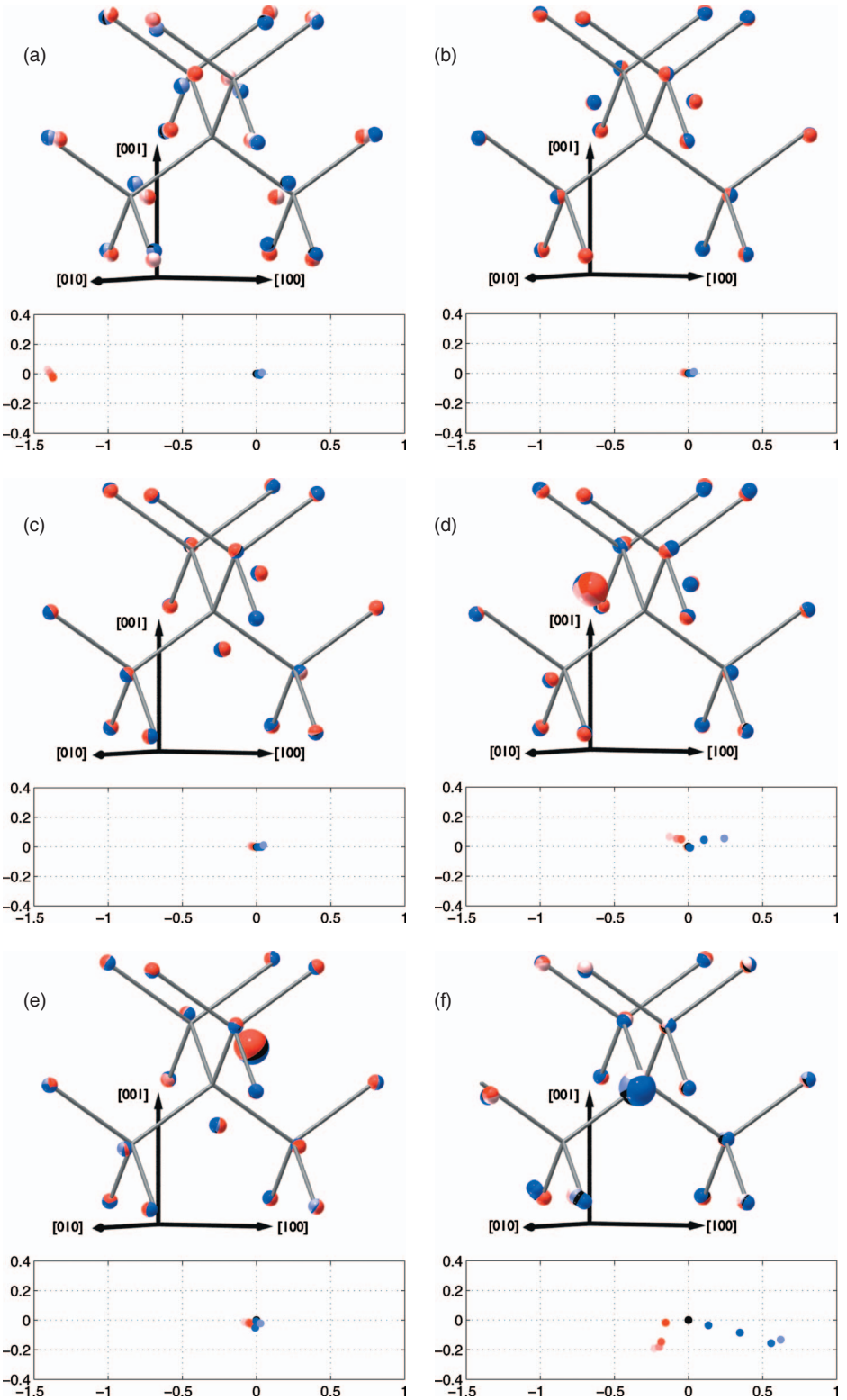

FIG. 2. (Color) The minimum energy configurations of the mobile defects in real (upper) and reduced configuration (lower) space. The saturation of the colors for compressive (red) and tensile (blue) strain increases for values toward the unstrained case (black). The axis unit of the configuration space is given in Angström. The As atom is represented by a larger sphere.

lations. We performed a MD simulation of 170 ps at 1000 °C. Our result confirmed the ring mechanism proposed in other studies.[19,20] After the MD simulation, start and end configurations of the appropriate migrations were determined with relaxations from corresponding MD steps. The migration barriers between these configurations were finally calculated with NEB simulations [Fig. 4(a)]. They are in the same range as those of other *ab initio* studies.[19,20] Starting from the

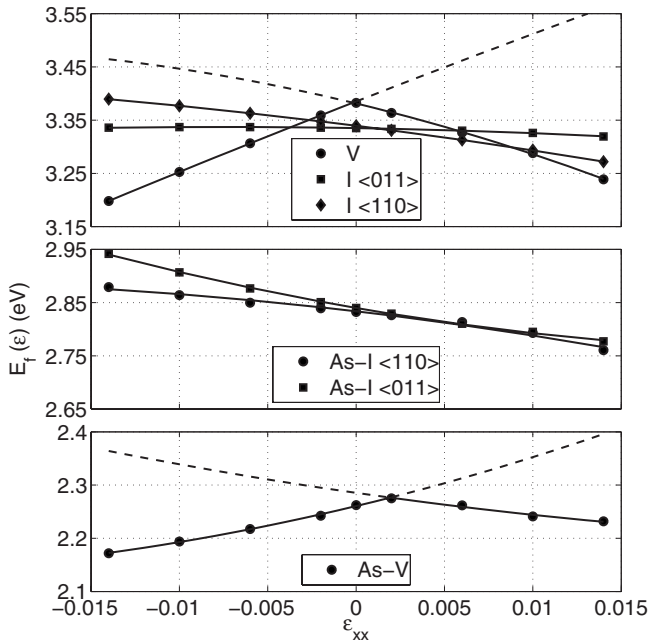

FIG. 3. The calculated formation energies (markers) of the mobile defects *V*, *I*, As-*I*, and As-*V* with quadratic fits (lines).

preferred minimum energy configuration NN1, the exchange event was most frequent (Table I) due to its smallest energy barrier (0.70 eV). Although the NN2 configuration was visited several times, only 4.6 ps were spent in this configuration. In most of the cases when *V* jumped to the NN2 position, it immediately moved back into the NN1 configuration as a consequence of the small backward barrier (0.01 eV). The time spent in the NN3 configuration was even shorter (1.4 ps).

The trajectories for the three migrations are presented in Figs. 4(b)–4(d). During the exchange the As atom moves straight into the vacancy position. The silicon atom deviates only slightly from the direct path when moving from NN3 to NN2 [Fig. 4(d)]. However, during the migration of *V* from NN1 to NN2, the corresponding silicon atom does not move on the shortest line from one lattice site to the next. It passes a position with a small kink in the energy plot and finally ends in a configuration slightly off a lattice site, shifted into the direction of *V*. This is caused by the two cumulative

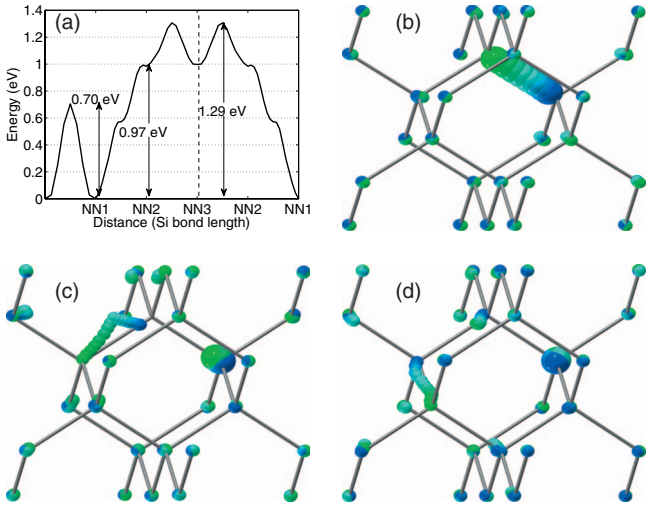

FIG. 4. (Color) Energy barriers (a) and migration trajectories (b)–(d) of the ring mechanism calculated with NEB simulations. For consecutive NEB images the atoms are colored from green to blue. The As atom is indicated by a larger sphere.

effects that *V* acts attractive on its neighbors whereas the As atom repels surrounding silicon atoms.

D. As-*V* diffusion in strained silicon

As a next step toward the determination of the As-*V* diffusion coefficient in uniaxially strained silicon, the diffusion rate $\Gamma_{\text{As-}V}(\varepsilon)$ for the ring mechanism was calculated with a simple random walk model where *V* jumps between the minimum energy configurations. As all possible orientations of the ring mechanism are symmetrically equivalent in [100]-uniaxially strained silicon, we assume As-*V* to diffuse isotropic. We considered the most probable case where *V* moves directly around the hexagonal ring, i.e., it was forbidden to jump into previous configurations,

$$\Gamma_{\text{As}-V}(\varepsilon) = \left(\sum_{i=1}^{5} \frac{1}{\Gamma_i(\varepsilon)} \right)^{-1} \prod_{i=1}^{5} \left(\frac{\Gamma_i(\varepsilon)}{\Gamma_i(\varepsilon) + \Gamma_{i^{-1}}(\varepsilon)} \right). \quad (4)$$

Here, $\Gamma_i(\varepsilon) = \Gamma_a e^{-E_b^i(\varepsilon)/kT}$ is the rate for migration i and i^{-1} denotes the backward migration.[21] The attempt frequency Γ_a

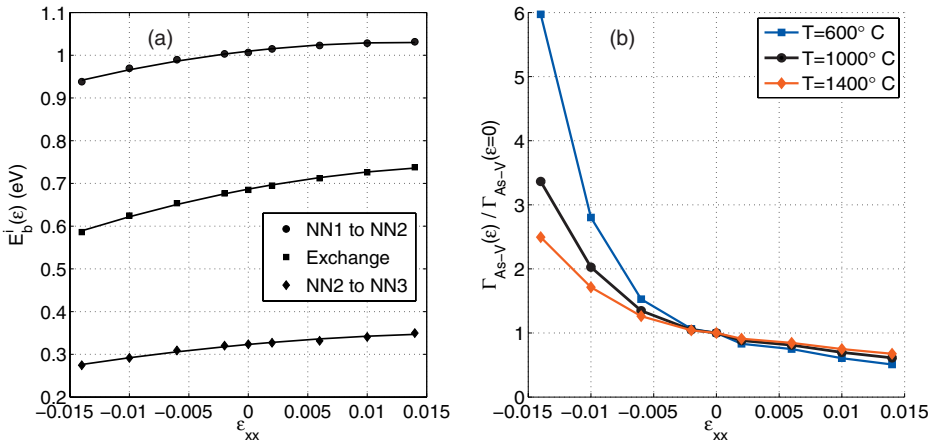

FIG. 5. (Color) Left: the quadratically fitted dominant energy barriers for the migrations of the As-*V* ring mechanism. Right: The relative diffusion rate for three different annealing temperatures.

was assumed to be the same for all migrations and strains. The correctness of this assumption is based on calculations of the attempt frequency using strain-dependent transition state theory. We found that their influence on $\Gamma_i(\varepsilon)$ is at least a factor of 100 smaller than that of the energy barriers. In any case, when the relative diffusion rate is finally calculated, Γ_a cancels out. $E_b^i(\varepsilon)$ is the energy barrier of migration i and k and T are the Boltzmann constant and the temperature, respectively. To complete our estimation of the diffusion coefficient we included the calculated As-V formation energies

$$D_{\text{As-}V}(\varepsilon) = D_0 e^{-E_f^{\text{As-}V}(\varepsilon)/kT} \Gamma_{\text{As-}V}(\varepsilon), \tag{5}$$

where the prefactor D_0 with dimension (cm^2) was assumed to be strain independent.

The results for the NEB barriers and the relative diffusion rate are presented in Fig. 5. The strain dependent NEB simulations were based on the MD simulation. To determine the start and end configurations, the minimum energy configurations of the MD simulation were again relaxed in strained silicon. Besides the already discussed NN1 configuration of As-V, also the other ring configurations showed small changes for the different strains. As the high barriers dominated in the calculation of $\Gamma_{\text{As-}V}(\varepsilon)$, only those are shown. In contrast to the result of an *ab initio* study with biaxial strain,[5] we found a stronger strain dependence of the relative diffusion rate in compressive silicon than in tensile.

The final result for the relative diffusion coefficient calculated with Eq. (5) is shown in Fig. 6. In qualitative agreement with hydrostatic pressure experiments,[22] for compressive strain and an annealing temperature of 1000 °C, diffusion is strongly enhanced (by a factor of up to 8) compared to unstrained silicon. This fact is a direct consequence of the increasing diffusion rate and the decreasing formation energy in Fig. 3, both contributing to enhanced diffusion. For the same reasons there is no relevant change of As diffusion in tensile strained silicon because the decreasing diffusion rate cancels the increasing concentration. This result again agrees with an experimental investigation.[23] The same trend is observed for other temperatures. For the compressive case

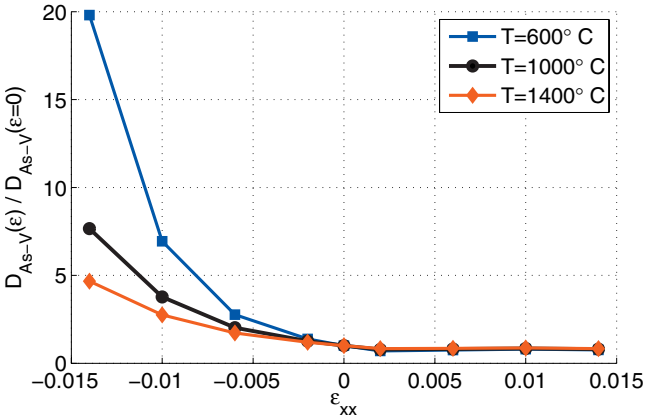

FIG. 6. (Color) The relative diffusion coefficient of As-V in strained silicon.

and T=600 °C, our results predict diffusion enhancement by a factor of 20. For high temperatures (T=1400 °C), the increase is comparatively smaller, and we predict a factor of 4.7.

III. CONCLUSION

To summarize, we established a strong increase of As diffusion in uniaxially compressive silicon due to increasing As-V concentration and lowered migration barriers. In the tensile case, these two quantities showed opposite strain dependence, with the result that diffusion remained unchanged. Next to the results, the strength of this work is the developed methodology that combines a sequence of absolutely indispensable computation steps. Our method is perfectly suited for further investigations on point defect diffusion in strained silicon.

ACKNOWLEDGMENTS

This work was supported by a grant from the Swiss National Supercomputing Centre CSCS and the research project was supported by the Swiss innovation promotion agency CTI.

[1] D. Nobili, S. Solmi, A. Parisini, M. Derdour, A. Armigliato, and L. Moro, Phys. Rev. B **49**, 2477 (1994).
[2] M. Ramamoorthy and S. T. Pantelides, Phys. Rev. Lett. **76**, 4753 (1996).
[3] J. Xie and S. P. Chen, Phys. Rev. Lett. **83**, 1795 (1999).
[4] S. E. Thompson, G. Sun, Y. S. Choi, and T. Nishida, IEEE Trans. Electron Devices **53**, 1010 (2006).
[5] S. T. Dunham, M. Diebel, C. Ahn, and C. L. Shih, J. Vac. Sci. Technol. B **24**, 456 (2006).
[6] G. Kresse and J. Hafner, Phys. Rev. B **47**, 558 (1993).
[7] G. Kresse and J. Furthmüller, Phys. Rev. B **54**, 11169 (1996).
[8] G. Kresse and D. Joubert, Phys. Rev. B **59**, 1758 (1999).
[9] J. J. Wortman and R. A. Evans, J. Appl. Phys. **36**, 153 (1965).
[10] W. M. Lai, D. Rubin, and E. Krempl, *Introduction to Continuum Mechanics* (Butterworth, Washington, DC/Heinemann, London, 1999).
[11] D. R. França and A. Blouin, Meas. Sci. Technol. **15**, 859 (2004).
[12] I. Borg and P. Groenen, *Modern Multidimensional Scaling: Theory and Applications* (Springer, New York, 2005).
[13] K. Vollenweider, B. Sahli, and W. Fichtner, Phys. Rev. Lett. **103**, 075503 (2009).
[14] B. Sahli, K. Vollenweider, and W. Fichtner, Phys. Rev. B **80**, 075208 (2009).
[15] M. Diebel, Ph.D. thesis, University of Washington, 2004.
[16] P. Pichler, *Intrinsic Point Defects, Impurities, and their Diffusion in Silicon* (Springer-Verlag, Wien, 2004).
[17] A. Ural, P. B. Griffin, and J. D. Plummer, J. Appl. Phys. **85**, 6440 (1999).

[18] O. Sugino and A. Oshiyama, Phys. Rev. B **46**, 12335 (1992).
[19] O. Pankratov, H. Huang, T. Diaz de la Rubia, and C. Mailhiot, Phys. Rev. B **56**, 13172 (1997).
[20] J. Zhang, Y. Ashizawa, and H. Oka, J. Phys.: Condens. Matter **18**, 4879 (2006).
[21] For example, if i denotes the migration of V from NN1 to NN2, then i^{-1} is the inverse migration from NN2 to NN1.
[22] E. Nygren, M. J. Aziz, and D. Turnbull, Appl. Phys. Lett. **47**, 105 (1985).
[23] N. Sugii, S. Irieda, J. Morioka, and T. Inada, J. Appl. Phys. **96**, 261 (2004).